Polymorphisms in human dopamine D2 receptor gene affect gene expression, splicing, and neuronal activity during working memory

Ying Zhang*, Alessandro Bertolino†, Leonardo Fazio†, Giuseppe Blasi†, Antonio Rampino†, Raffaella Romano†, Mei-Ling T. Lee‡, Tao Xiao‡, Audrey Papp*, Danxin Wang*, and Wolfgang Sadée*§¶

*Program in Pharmacogenomics, Department of Pharmacology, §Department of Psychiatry, Division of Human Genetics, College of Medicine, and College of Pharmacy, and ‡Division of Biostatistics, College of Public Health, Ohio State University, Columbus, OH 43210; and †Group of Psychiatric Neuroscience, Department of Neurology and Psychiatry, University of Bari, 70124 Bari, Italy

Edited by Edward G. Jones, University of California, Davis, CA, and approved October 25, 2007 (received for review July 29, 2007)

Subcortical dopamine D2 receptor (DRD2) signaling is implicated in cognitive processes and brain disorders, but the effect of *DRD2* variants remains ambiguous. We measured allelic mRNA expression in postmortem human striatum and prefrontal cortex and then performed single nucleotide polymorphism (SNP) scans of the *DRD2* locus. A previously uncharacterized promoter SNP (rs12364283) located in a conserved suppressor region was associated with enhanced DRD2 expression, whereas previously studied *DRD2* variants failed to affect expression. Moreover, two frequent intronic SNPs (rs2283265 and rs1076560) decreased expression of DRD2 short splice variant (expressed mainly presynaptically) relative to DRD2 long (postsynaptic), a finding reproduced *in vitro* by using minigene constructs. Being in strong linkage disequilibrium with each other, both intronic SNPs (but not rs12364283) were also associated with greater activity of striatum and prefrontal cortex measured with fMRI during working memory and with reduced performance in working memory and attentional control tasks in healthy humans. Our results identify regulatory *DRD2* polymorphisms that modify mRNA expression and splicing and working memory pathways.

allelic expression imbalance | splice variant | promoter polymorphism | brain imaging

Although genetic factors contribute to central nervous system (CNS) disorders, only a few genes have been identified as unequivocal risk factors. Aberrant subcortical dopamine D2 receptor (DRD2) signaling is implicated in brain disorders such as drug addiction (1, 2), schizophrenia, and Parkinson's disease (3, 4). *DRD2* variants Taq1A, promoter polymorphism −141C del/ins, and a synonymous SNP in exon 7 (C957T) have been associated with schizophrenia and drug abuse (5–8), but associations are not consistently replicated (9–11). Moreover, polymorphisms relevant *in vivo* remain unknown. Our goal was to identify functional *DRD2* polymorphisms linked to CNS functions.

DRD2 variants could have maximal impact in the basal ganglia endowed with prominent DRD2 signaling. A crossroad between cortex and dopamine projections from the brainstem, basal ganglia in the caudate and pallidum mediate cognitive processes (12–14) and contribute to focus of working memory (15). Dopamine–DRD2 signaling in these structures decreases GABA (16, 17) and glutamate inputs to striatal spiny neurons (18). DRD2 density affects working memory performance in mice (19), and striatal DRD2 receptor availability is linked to working memory and attention in humans (20). Another mechanism modulating DRD2 signaling involves alternative splicing of exon 6 to yield DRD2L (long) and DRD2S (short, considered an autoreceptor), expressed mainly postsynaptically and presynaptically, respectively (21, 22). Relative expression of DRD2S and L is critical to dopamine modulation of GABA and glutamate striatal transmission (23, 24).

We searched for genetic variants modulating DRD2 neurotransmission in human brain. Because the *DRD2* locus lacks frequent nonsynonymous SNPs that alter receptor function, we focused on regulatory polymorphisms affecting gene transcription and mRNA splicing, using allelic expression analysis in human postmortem brain tissues. Allelic expression imbalance (AEI), an indicator of *cis*-acting regulatory polymorphisms (25–29), led to discovery of a regulatory promoter SNP and two SNPs affecting DRD2 splicing associated with differential activity in the working memory network and cognitive performance in healthy humans.

Results

Allelic DRD2 Expression in Human Brain and SNP Scanning. Detection of different mRNA expression from each allele (AEI) requires use of marker SNPs located in transcribed regions, to compare allelic ratios in genomic DNA and mRNA (as cDNA). Using a PCR-primer extension analysis (SNaPshot), we measured allelic DRD2 expression in 68 autopsy tissue samples (54 from prefrontal cortex, 14 from striatum) heterozygous for at least one of three marker SNPs (SNP20 and SNP21 in exon 7, and SNP22 in 3′-UTR) [Table 1 and supporting information (SI) Fig. 6]. Results obtained independently with two marker SNPs in compound heterozygotes were highly correlated (r = 0.93–0.96) (SI Fig. 7), supporting assay validity. Significant AEI was found in 15 tissues with ratios below and above unity (Fig. 1), suggesting a regulatory polymorphism not in linkage disequilibrium with the marker SNPs.

To scan for regulatory *DRD2* polymorphism, we genotyped 23 SNPs in all samples (SNP1–23; Table 1). Predicted haplotype frequencies and pairwise linkage D′ scores (SI Table 2 *a* and *b*) are consistent with previous studies, showing a strong haplotype block 3′ of exon 2. A single promoter region SNP (at −844) was strongly linked to AEI (SNP2, rs12364283; P = 0.001, adjusted P = 0.023) (SI Table 3). A two-loci genetic analysis with HelixTree (Golden Helix) did not further strengthen the association, suggesting that SNP2 is the sole polymorphism contributing to AEI (adjusted $P = 9.74 \times 10^{-5}$, SI Fig. 8*a*). Moreover, removal of subjects heterozygous for SNP2 failed to reveal a significant association of any other SNPs with AEI (SI Fig. 8*b*). Specifically, marker SNP21, possibly affecting mRNA stability (30), promoter SNP4 (−141C del/ins) (rs1799732) (6), and SNP14 in intron 2 (31), were not associated with the observed allelic ratios. In addition, we identified 10 variants of a GAA/GAAA repeat region located 3′ of SNP2 (SI Table 4),

Author contributions: Y.Z., A.B., and W.S. designed research; Y.Z., L.F., G.B., A.R., R.R., and D.W. performed research; Y.Z., A.B., L.F., G.B., A.R., R.R., M.-L.T.L., T.X., A.P., D.W., and W.S. analyzed data; and Y.Z., A.B., M.-L.T.L., and W.S. wrote the paper.

The authors declare no conflict of interest.

This article is a PNAS Direct Submission.

¶To whom correspondence should be addressed at: Department of Pharmacology, College of Medicine and Public Health, Ohio State University, 333 West 10th Avenue, Columbus, OH 43210-1239. E-mail: wolfgang.sadee@osumc.edu.

This article contains supporting information online at www.pnas.org/cgi/content/full/0707106104/DC1.

Table 1. Polymorphism of *DRD2*

SNP no.	SNP	Region (gene)	MAF Stanley	MAF U Bari
1	rs10891556	G/T 5′up	0.15	
2	rs12364283	T/C 5′up	0.07	0.05
3	re1799978	A/G Promoter	0.05	
4	rs1799732	C/−C Promoter	0.08	
5	rs4938019	T/C Intron 1	0.14	
6	rs4350392	C/A Intron 1	0.13	
7	rs4648317	C/T Intron 1	0.14	
8	rs4581480	T/C Intron 1	0.08	
9	rs12574471	C/T Intron 1	0.14	
10	rs4648318	A/G Intron 1	0.25	
11	rs7125415	C/T Intron 1	0.08	
12	rs7103679	C/T Intron 1	0.15	
13	rs1125394	A/G Intron 1	0.17	
14	rs2734836	G/A Intron 2	0.16	
15	rs2075654	G/A Intron 2	0.18	
16	rs12363125	A/G Intron 5	0.41	
17	rs2283265	G/T Intron 5	0.17	0.08
18	rs2511521	T/C Intron 5	0.24	
19	rs1076560	G/T Intron 6	0.17	0.10
20	rs6275	C/T Exon 7	0.28	
21	rs6277	C/T Exon7	0.46	
22	rs6279	C/G 3′UTR	0.28	
23	rs1800497	C/T 3′down	0.18	

Allele frequencies were calculated from the 105 samples of The Stanley Foundation (prefrontal cortex). Allele frequencies in the cohort of 117 subjects from the University of Bari are also provided where available.

also not significantly correlated with AEI (adjusted $P = 0.31$), arguing against a role in transcription.

Overall, mRNA expression levels did not correlate with genotype of any tested SNP (data not shown), probably because of greater noise observed in total mRNA levels compared with allelic expression ratios. These results indicate that promoter SNP2 (rs12364283 in position −844) affects expression of DRD2 mRNA.

Reporter Gene Assay of SNP2 (rs12364283). We tested *DRD2* promoter fragments of different lengths (Pro_S, Pro_M, Pro_L) in a luciferase reporter plasmid (Fig. 2). Only Pro_L contained SNP2 (T/C alleles, −844) and the GAA/GAAA repeat region, resulting in four Pro_L variants containing T/C alleles and two repeat variants (360 and 364 nucleotides). Shown in Fig. 2, Pro_S and Pro_M displayed greater promoter activities than Pro_L fragments in both HEK293 and SH-SY5Y cells, revealing a silencer domain within −600 to −963. However, the C allele (minor) of SNP2 significantly enhanced promoter activity over the T allele in both cell lines. The GAA/GAAA repeat variants had no

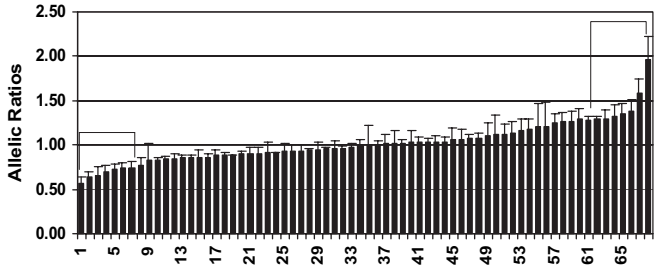

Fig. 1. Allelic DRD2 mRNA expression ratios in 54 prefrontal cortex and 14 striatum samples heterozygous for at least one marker SNP, SNP20 (T/C; 47 subjects), SNP21 (C/T; 54 subjects), and SNP22 (C/G; 49 subjects). Ratios were normalized to DNA and are mean ± SD (two cDNA syntheses and six PCRs per sample). For subjects heterozygous for more than one marker SNP, ratios obtained with SNP21 were used, whereas SNP20 was used as marker in samples homozygous for SNP21. The brackets show samples with significant AEI.

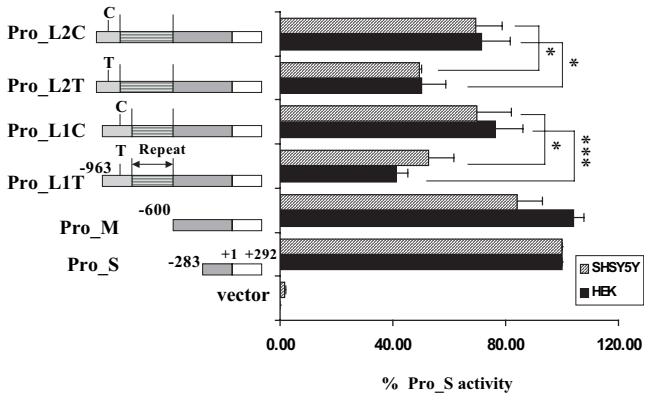

Fig. 2. Luciferase assay of *DRD2* promoters in HEK-293 and SH-SY5Y cells. The minor C allele of SNP2 conferred higher promoter activity than the T allele in both cell lines, regardless of GAA/GAAA repeat variants (*, $P < 0.05$, and ***, $P < 0.0001$, one-way ANOVA, Bonferroni's multiple comparison test).

effect, consistent with results from allelic mRNA ratios. We conclude that promoter SNP2 affects DRD2 expression, the minor C allele displaying greater expression.

Expression of DRD2 Splice Variants in Prefrontal Cortex and Striatum. To test for genetic effects on splicing, we measured allele-specific expression for each splice variant (DRD2L and DRD2S) (SI Fig. 9*a*). Of 37 tissues analyzed, 20 displayed substantial differences in allelic mRNA expression ratios between DRD2S and DRD2L, indicating a frequent polymorphism affecting splicing (SI Fig. 9*a*). Allelic mRNA ratios of the two splice variants were consistent with the mean allelic ratios measured independently for total DRD2 mRNA, supporting the accuracy of the assays.

Scanning the *DRD2* locus for SNPs linked to allelic splicing differences revealed a strong association with SNPs in a 3′-haplotype block (SNP12–15, -17, -19, and -23), with SNP17 and SNP19 (in complete linkage disequilibrium) displaying the lowest *P* value (adjusted $P = 5.2 \times 10^{-8}$, SI Fig. 9*b*). The location of SNP17 and -19 in introns 5 and 6 is consistent with a role in exon 6 splicing. Also located in intron 5, SNP16 and -18 were not significantly associated with splicing and therefore not further studied. Tissues heterozygous for SNP17/19 yielded significantly lower allelic ratios for DRD2S compared with DRD2L (Fig. 3*a*). Considering the linkage relationship between SNP17/19 and marker SNP21, the minor T alleles of SNP17/19 favor inclusion of exon 6, resulting in a significant reduction of the DRD2S splice variant.

To confirm this result, we measured relative expression of DRD2S and DRD2L mRNA in prefrontal cortex and striatum by using PCR with fluorescently labeled primers. As reported (21), relative DRD2S mRNA expression was higher in prefrontal cortex ($34 \pm 7\%, n = 98$) than in striatum ($9.5 \pm 6.1\%, n = 25$) ($P < 0.0001$ (Student's *t* test; SPSS). Grouping of the subjects by genotype (GG vs. GT+TT of SNP17/19) revealed that T carriers had significantly less relative DRD2S mRNA expression than GG carriers, both in prefrontal cortex and in striatum (Fig. 3*b*), confirming the results obtained with allele-specific analysis of the splice variants. Overall DRD2 mRNA levels were considerably higher in striatum compared with prefrontal cortex (SI Fig. 10) but were not significantly different when grouped by SNP17/19 genotype (data not shown).

Alternative Splicing of a DRD2 Minigene. We constructed a partial gene, containing exon 5 to exon 7, in an expression vector (Fig. 4). Four minigene constructs carrying all possible allele combinations for SNP17/19 (G–G, T–T, T–G, and G–T) were transfected into HEK-293 cells, and percentage DRD2S of total DRD2 mRNA levels was determined. As in brain tissues, the minor T alleles for both intronic SNPs generated significantly less DRD2S than the G

NEUROSCIENCE

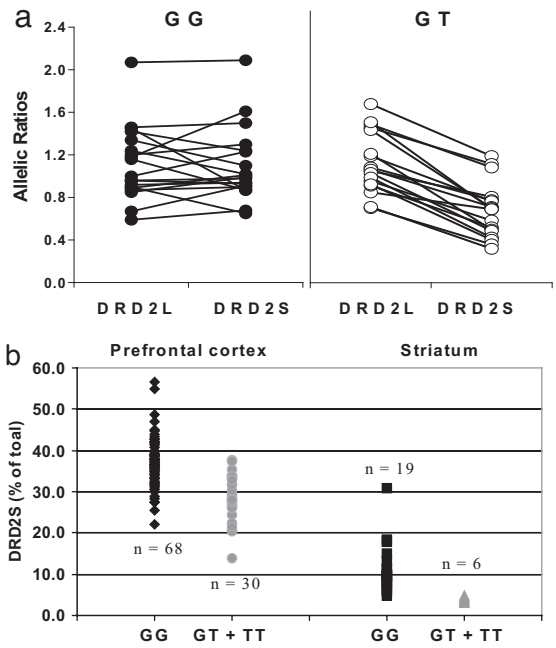

Fig. 3. Allelic mRNA ratios of DRD2L and DRD2S grouped by SNP17/19 genotype. (*a*) Allelic ratios for DRD2L and DRD2S from the same subject are connected by solid lines. (*b*) Expression of DRD2S mRNA grouped by SNP17/19 genotypes (GG vs. GT + TT) in prefrontal cortex and striatum. Data are mean ± SD, $n = 3$, $P < 0.001$ [prefrontal cortex, $F = 18.70$, $P < 0.0001$, $n = 40$; in striatum, $F = 10.92$, $P = 0.003$, $n = 25$ (one-way ANOVA)].

allele (Fig. 4). Moreover, a single T allele in either of the two intronic SNPs also significantly reduced the formation of DRD2S compared with the G–G haplotype, indicating that both SNPs affect splicing. We did observe the formation of further splice isoforms in addition to S and L in HEK-293 cells, both from endogenously expressed DRD2 and from the transfected minigenes (measured with PCR primers specific for each). The splice patterns of endogenous and minigene DRD2 were similar, suggesting that the minigene contains the needed elements for *cis*-regulation of splicing. The significance of additional splice variants in nonneuronal tissues remains to be studied. These results indicate that both minor alleles of SNP17 and -19 reduce formation of DRD2S.

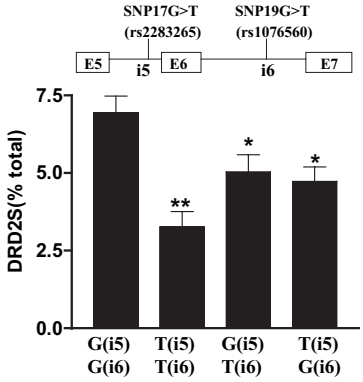

Fig. 4. Alternative splicing from *DRD2* minigenes in HEK-293 cells. Minigenes carrying SNP17 and -19 [G(i5)/G(i6), T(i5)/T(i6), G(i5)/T(i6), T(i5)/G(i6)] were transfected into HEK cells and DRD2S expression measured relative to total DRD2 mRNA. Data are mean ± SD ($n = 6$). The four haplotypes also carry two additional SNPs (SNP16G > A and SNP21C > T) not associated with alternative splicing (SI Fig. 9*b*). *, $P < 0.05$, **, $P < 0.01$, ANOVA with Dunnett posttest, compared with G(i5)/G (i6).

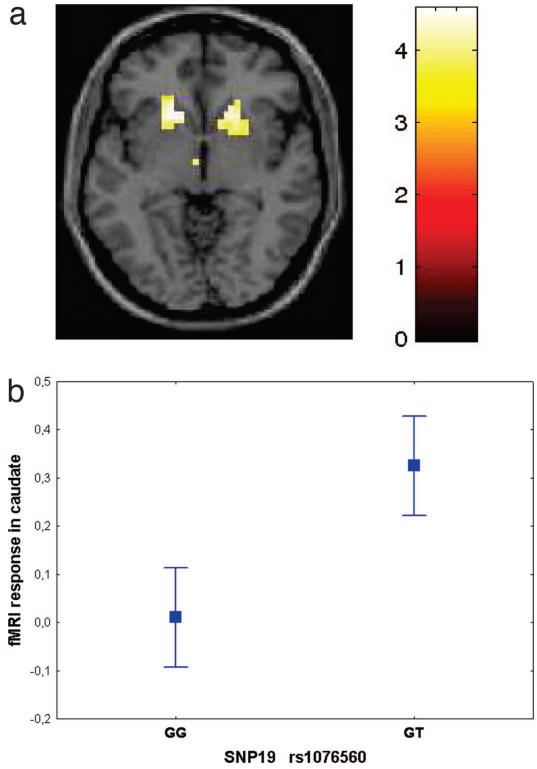

Fig. 5. SNP19 genotype analysis of fMRI response during working memory. (*a*) Results of ANOVA in SPM2 overlaid on an average axial MRI at the level of the head of the caudate. The color bar indicates *z* values of the difference in BOLD signal between the groups separated by GG and GT genotype. During the working memory task, GT subjects had greater BOLD activity in bilateral head of caudate than GG subjects. (*b*) Mean ± 0.95 standard error plots reflecting percent signal change from the cluster in left caudate head. Subjects with GT genotype had greater engagement of caudate head compared with GG subjects (one way ANOVA, $F(1, 42) = 18.950$, $P = 0.00008$).

Functional Imaging Data and DRD2 Genotype. We next tested the physiological relevance of SNP2, -17, and -19 in healthy humans undergoing fMRI measurements during the N-Back task, with particular attention to striatal regions where DRD2 signaling is prominent. For each of SNPs 2, 17, and 19, we identified heterozygous carriers (17, 17, and 22 subjects, respectively) and matched them with an equal number of subjects homozygous for the main allele. None of the subjects were homozygous for the minor alleles. ANOVAs and χ^2 showed no significant differences between genotype groups in any demographic variable ($P > 0.1$) (SI Table 5*a*). ANOVAs on behavioral data confirmed that subjects included in fMRI analyses were matched on accuracy and reaction time on the N-Back task ($P > 0.1$). Analysis of the working memory fMRI imaging data in the whole sample revealed significant blood oxygen level-dependent (BOLD) responses in the cortical and subcortical network, including dorsolateral prefrontal cortex (BA 9), anterior cingulate (BA 24 and BA 32), premotor area (BA 6), parietal cortex (BA 39/40), caudate, and putamen, consistent with earlier reports (32–39).

Testing for genotype effects, ANOVA of the promoter SNP2 did not indicate any statistically significant difference in any brain region. On the other hand, ANOVA of the fMRI data revealed a highly significant effect of intron 6 SNP19 genotype: the G/T genotype was associated with greater BOLD activity than the GG genotype in bilateral head of the caudate, left middle frontal gyrus, left precentral gyrus, left anterior cingulate, left thalamus, left superior frontal gyrus, and left caudate tail (Fig. 5 and SI Table 6).

The GT genotype of intron 5 SNP17 was similarly associated with

greater activity than GG in caudate, left claustrum, inferior frontal gyrus, left superior temporal gyrus, and right posterior cingulate (SI Table 6). No significant difference was found for the inverse contrast (G/G > G/T) for both SNP17 and -19. These results suggest that intronic SNP17 and -19 robustly modulate activity of the working memory network, especially striatal firing.

Behavioral Cognitive Data and DRD2 Genotype. Cognitive assessment included the N-Back working memory task ($n = 117$) and the variable attentional control (VAC) task ($n = 105$), which rely heavily on prefronto-striatal circuits (for demographics see SI Table 5*b*). A repeated measures ANOVA of the N-Back data indicated an SNP17 interaction with working memory load ($F_{1,113} = 8.3, P = 0.004$) (SI Fig. 11*a*). Post hoc analysis with least significant difference (LSD) showed that heterozygote subjects have significantly reduced performance at 2-Back compared with homozygotes ($P = 0.02$). Similar but statistically not significant trends were found for SNP19 ($F_{1,109} = 1.8, P = 0.1$).

A repeated measures ANOVA of the VAC data (attention measure) also supported an SNP17 interaction with cognitive load ($F_{2,206} = 2.8, P = 0.05$) (SI Fig. 11*b*). Post hoc analyses indicated that heterozygote subjects have reduced performance at the highest load of attentional control compared with homozygote subjects ($P = 0.03$). Similar results were evident for SNP19 at the highest load ($F_{2,198} = 3.3$, $P = 0.03$) (SI Fig. 11*b*), with heterozygotes performing worse than homozygotes (post hoc analysis, $P = 0.01$).

Consistent with the fMRI data, SNP2 genotype did not have any statistically significant effect on performance of the N-Back or of the VAC tasks (all $F < 0.8$, all $P > 0.4$).

Discussion

This study reveals regulatory polymorphisms in dopamine receptor *DRD2*. Allelic mRNA expression analysis of human brain autopsy tissues, SNP scanning of the *DRD2* locus, and reporter gene and minigene experiments identified one upstream promoter polymorphism and two intronic SNPs affecting DRD2 splicing. Moreover, genotype-driven changes in DRD2 splicing robustly affected behavioral performance and activity of the working memory network in humans, especially in the striatum rich in dopamine projections and DRD2 receptors.

The promoter SNP2, located −844 bp upstream of the transcription start site, significantly affects allelic mRNA expression of DRD2, supporting a regulatory role in human brain. Although both rat and human *DRD2* contain a promoter region at approximately −300 bp (6, 40), sequences further upstream often contain regulatory domains (40, 41). Our reporter gene results reveal a repressor region, located between −600 and −963 bp (6), which could mask effects of the previously proposed promoter SNP4 (−141 Ins/Del) *in vivo* (6). Importantly, the minor C allele of SNP2 confers higher transcriptional activity compared with the major T allele, indicating a gain-of-function, potentially a penetrant property even in heterozygotes. Conserved sequences flanking SNP2 contain putative sites for transcription factors, such as E47, ANF, NF-X3, and HSF1, whereas the C allele lacks ANF and HSF1 binding sites but generates a new AREB6 site (TRANSFAC, version 8.3) (42) (SI Fig. 12). Detailed molecular studies are needed to resolve the regulatory events. Because SNP2 accounts for only part of the observed AEI ratios, possible contributions from epigenetic factors need to be investigated.

A second striking finding is the discovery of intronic SNP17 and -19 flanking exon 6, linked to DRD2 splicing. Whereas *trans* regulation can account for splicing differences between prefrontal cortex and striatum (21), analysis of allelic expression for each splice variant demonstrated an additional role for *cis*-acting polymorphisms. Both SNP17 and SNP19 modulate putative splice factor (SRP protein) binding sites, with SNP17 G allele generating an SRP55 site and T alleles forming SC35 (SNP17) and SRP40 (SNP19) sites [ESE finder (43)]. Minigene experiments confirmed that the minor alleles produce significantly less DRD2S than the major alleles. Although SNP17 and SNP19 are tightly linked to each other, minigene experiments also indicate that both SNP17 and -19 affect splicing individually (Fig. 4). Taken together, the T alleles of SNP17/19 reduce formation of the S variant in favor of the L variant.

Previously suggested *DRD2* polymorphisms appear not to contribute directly to mRNA expression and splicing. These variants include promoter SNP4 (−141 Ins/Del) (6) and a putative regulatory SNP14 in intron 2 (31), exonic SNP21 (C957T) shown to alter mRNA turnover rate *in vitro* (30), and SNP23 located distantly 3′-downstream (Taq1A) (SI Fig. 6). Yet, SNP23 had been associated with reduced DRD2 density *in vivo* (44), with various CNS disorders and treatment outcomes (45). We show here that SNP23 Taq1A1 allele is in linkage disequilibrium ($D' = 0.855$) with the minor allele of the intronic SNP17/19, providing a mechanistic basis for the clinical associations observed with Taq1A.

To test the relevance of these *DRD2* polymorphisms, we measured brain activity and working memory in normal human subjects. Promoter SNP2 failed to affect brain activity and working memory or attentional control performance. Two factors could account for this negative result. First, SNP2 accounts for only a portion of the allelic expression differences observed in our study. Second, SNP2 is expected to affect overall DRD2 density, rather than splice variant L/S ratios, the latter potentially having a stronger effect on neuronal firing. However, penetrance of this SNP may be revealed when analyzing larger cohorts or different phenotypes.

The fMRI results obtained in subjects matched for memory performance did reveal robust associations between both intronic SNP17 and -19 with activity of the ventral striatum, thalamus, dorsolateral prefrontal cortex, and premotor cortex during working memory. Minor allele carriers had greater activity in these brain regions although accuracy and reaction time were not significantly different, suggesting greater energy expenditures for similar task performance. To evaluate performance in prefronto-striatal-mediated tasks, tapping into working memory and attentional control, we genotyped additional subjects with whom only the memory tasks were performed. The results indicate that both SNP17 and -19 have a behavioral effect, with heterozygotes performing worse, showing that altered DRD2 splicing appears to affect working memory and attentional control at high task loads.

These results are consistent with the known role of dopamine and DRD2 modulating the cortico-striato-thalamo-cortical network. Whereas the overall DRD2 receptor number modulates GABA-mediated inhibition of striatal neurons, inhibition of glutamate release preferentially involves the DRD2S variant (23, 24). Thus, reduced DRD2S expression is expected to increase excitability of striatal medium spiny neurons. Consistent with these electrophysiology experiments in rodents, our results demonstrate that the minor alleles of SNP17/19 associated with low DRD2S expression are also associated with greater activity in human striatum and other regions during working memory. This observation, in turn, is associated with lower performance in cognitive/attentional tasks, a relationship observed in previous studies (46).

The approach presented here, identifying regulatory polymorphisms first and then testing associations with endophenotypes (fMRI) and cognitive performance, can reveal frequent regulatory variants that had escaped previous genetic analysis even in intensely studied genes such as *DRD2* (also see refs. 26–28). This approach represents a valuable complement to the emerging genome-wide association studies that generate numerous candidate genes but no indication of the functional variants. *DRD2* has already been the subject of numerous clinical association studies because of its perceived importance in CNS disorders. The regulatory *DRD2* polymorphisms identified here could affect not only cognitive processes but also brain disorders, including schizophrenia and drug addiction.

Materials and Methods

Postmortem Human Brain Tissues. One hundred five DNA and RNA samples, extracted from prefrontal cortex autopsy tissues (for details see *SI Materials and Methods*), were obtained from The Stanley Medical Research Institute's (Chevy Chase, MD) brain collection, courtesy of M. B. Knable, E. F. Torrey, M. J. Webster, and R. H. Yolken. DNA and RNA were extracted as described in ref. 26. cDNA was synthesized with reverse transcriptase II (Invitrogen) by using both gene-specific primers and oligo(dT).

Genotyping Methods. Spanning the *DRD2* locus, 23 SNPs were genotyped in 105 prefrontal cortex samples. SNP2, -17 and, -19 were also genotyped for DNA samples from the University of Bari. SNPs were analyzed with allele-specific PCR primers as described in ref. 47 or SNaPshot (Applied Biosciences) (26). SNP13 and SNP15 were also genotyped with SNPlex (Applied Biosciences). PCR and SNaPshot primers are shown in SI Table 7*a*. SNP21 and SNP22 were genotyped with SNPlex and SNaPshot, and SNP20 was genotyped with allele-specific primers and SNaPshot, yielding identical results for both methods ($n = 105$). The GAA/GAAA variable repeat region was analyzed by using fluorescently labeled PCR primers (SI Table 7*b*) on an ABI 3730 sequencer (Applied Biosciences).

DRD2 mRNA Levels by Real-Time RT-PCR. RT-PCR was performed with β-actin as control, using 50 ng of cDNA, 200 nM primers (as used for SNP20, SI Table 7*a*), SYBR-Green, and AmpliTaq Gold and AmpErase UNG on an ABI 7000 (Applied Biosciences) (27). Cycle thresholds of DRD2 mRNA were normalized to β-actin. Cycle thresholds were also measured for GADPH mRNA, yielding similar results compared with β-actin ($r^2 = 0.703$).

Quantitative Detection of Splice Isoforms. DRD2L and DRD2S were measured after PCR amplification by using a Fam-labeled exon 5 forward primer and an exon 7 reverse primer (SI Table 7*b*) on an ABI 3730 (Applied Biosciences), as described in ref. 48. Standard curves were constructed by using varying mixtures of cloned DRD2L and S cDNA (SI Fig. 13 and SI Table 7*b*).

Allele-Specific DRD2 mRNA Expression. SNaPshot, a PCR/primer extension method (Applied Biosciences) (25–28), was applied to three marker SNPs located in transcribed regions (SNP20 and -21 in exon 7; SNP22 in 3′UTR) to measure allelic ratios of genomic DNA and mRNA (after conversion to cDNA). In brief, ≈100-bp fragments of DNA or cDNA flanking the SNPs were PCR amplified and SNaPshot reactions were performed (SI Table 7*a*). Reaction products were analyzed on an ABI 3730 (Applied Biosciences) with Gene Mapper software (Applied Biosciences). Allelic ratios of genomic DNA and cDNA were determined from peak areas and allelic cDNA ratios normalized to genomic DNA ratios, which varied within a narrow range (e.g., 0.96 ± 0.05 for SNP21). For assay validation, normalized allelic mRNA ratios were compared for two marker SNPs heterozygous in the same individual.

To determine allelic expression for DRD2S and DRD2L, each splice variant was separately amplified by using specific primers (SI Table 7*b*), and allelic mRNA expression ratios were measured with SNaPshot by using SNP21 and SNP20. Significant differences in allelic mRNA ratios between DRD2L and S reveal the presence of *cis*-acting splicing factors.

DRD2 Reporter Gene Assay. Promoter fragments were amplified from genomic DNA of two subjects heterozygous for SNP2 but homozygous for all other SNPs within the amplified regions (SI Table 7*b*) and cloned into PGL3_basic vector upstream of the luciferase gene by using KpnI and BglII cloning sites (Promega Biosciences). The constructs were transfected into HEK-293 and SH-SY5Y cells. The three DNA fragments were (short to long) Pro_S_ (−283 to + 292, as used by ref. 6), Pro_M (−600 to + 292), and Pro_L, (−963 to + 292; transcription start site +1) (49). Pro_L constructs contain a C or T allele of SNP2 (Pro_LC and Pro_LT) and two GAA/GAAA repeat variants (−806 to approximately −629). Pro_L was amplified from genomic DNA of two subjects homozygous for eight and four nucleotide deletions, respectively [repeat variants 360 (Pro_L1) and 364 (Pro_L2); SI Table 4] compared with reference variant 368. This amplification resulted in four constructs: Pro_L1T, Pro_L1C, Pro_L2T, and Pro_L2C (Fig. 2).

Cell Culture and Promoter Activity. Human embryonic kidney cells (HEK-293) and SH-SY5Y were cultured in DMEM/F12 media containing 10% FBS, penicillin (10 units/ml), and streptomycin (10 μg/ml) at 37°C with 5% CO_2. Twenty-four hours before transfection, $1–2 \times 10^5$ cells were planted into 24-well plates and transiently transfected with FuGENE HD Transfection Reagent (Roche Applied Science) in serum-free medium for 5 h. As control, *Renilla* luciferase constructs were cotransfected with PGL3 fused constructs at a 1:20 ratio. Cells were harvested after 48 h and transferred to 96-well plates, and luciferase activity was detected with Dual-Glo luciferase assays (Promega) on a fluorescence plate reader (PerkinElmer). Three independent transfections and duplicate luciferase assays were performed for each condition.

DRD2 Minigene Splicing. *DRD2* minigenes consisting of exons 5–7 and introns 5 and 6 were amplified from genomic DNA carrying G–G and T–T alleles of intronic SNP17 and 19. G–T and T–G haplotypes were generated with use of BamHI restriction site located between SNP17 and -19. The constructs were inserted downstream of the T7 promoter of pcDNA3 (Invitrogen) and sequenced, confirming the intended haplotypes plus two additional SNPs (SNP16 and -21) not associated with splicing (SI Fig. 9*b*). Minigene constructs were transfected into HEK-293 cells, and RNA was isolated after 45 h with TRIzol (Invitrogen). For cDNA synthesis, a plasmid-specific primer, SP6 (SI Table 7*b*), was used to avoid synthesis of endogenous *DRD2* cDNA. Splice variants were assayed by PCR with fluorescently labeled primers (SI Table 7*b*).

Statistical Analysis. Linkage disequilibrium between SNPs (expressed as D′) and haplotypes were calculated by using HelixTree (Golden Helix) (50). The presence of mRNA AEI was determined with normalized cDNA ratios (peak area ratios of cDNA/mean of the peak area ratios of DNA) by using Student's *t* test to assess deviation from unity in the mRNA ratios, with allelic mRNA ratios >1.2 or <1/1.2 (≈20%) as cutoff. Association between genotype status (heterozygous or homozygous) with AEI was tested with Fisher's exact tests and controlling for false discovery rates (51). Two-loci adjusted *P* values were calculated for the combination of any two SNPs by using HelixTree. To determine whether allelic expression differed between splice variants, we used a 1.25-fold difference in mRNA allelic ratios between DRD2L and DRD2S as cutoff.

Genotype Association with Cognition and Brain Activity. To examine the effect of genotypes on brain activity associated with working memory independent of sample size, demographic, or behavioral variation (potential confounds in fMRI analyses), we selected normal Caucasian subjects to control for these variables (SI Table 5*a*), divided equally into matched subjects homozygous for the main allele of each SNP and heterozygous subjects (homozygotes were not observed in the study). Subject numbers were 44 (SNP19) and 34 (SNP2 and SNP17). All 17 subjects heterozygous for SNP17 were also heterozygous for SNP19, whereas 5 subjects were heterozygous only for SNP19. Each SNP displayed Hardy–Weinberg equilibrium. One-way ANOVAs and χ^2 were used to evaluate the effects of genotype on demographics.

Working Memory Task for fMRI. During fMRI, all subjects completed a blocked paradigm of the N-Back task (33, 34). Briefly, ''N-Back'' refers to how far back in the sequence of stimuli the subject had to recall. The stimuli consisted of numbers (1–4) shown in random sequence and displayed at the points of a diamond-shaped box. A visually paced motor task served as a nonmemory-guided control condition (0-Back) that presented the same stimuli, but simply required subjects to identify the stimulus currently seen. In the working memory condition, the task required the recollection of a stimulus seen two stimuli previously (2-Back) while continuing to encode additional incoming stimuli. Performance was recorded as number of correct responses (accuracy) and reaction time.

Acquisition and Analysis of fMRI Data. Each subject was scanned by using a GE Signa 3T scanner (GE Healthcare with a standard head-coil. Echo planar imaging BOLD fMRI data were acquired as described in ref. 34 (echo time = 30 msec, repetition time = 2 sec, 20 contiguous slices, voxel dimensions = $3.75 \times 3.75 \times 5$ mm). We used a simple block design in which each block consisted of eight alternating 0-Back and 2-Back conditions (each lasting 30 sec), with 120 whole-brain scans obtained in 4 min and 8 sec. The first four scans were acquired to allow the signal to reach steady state and were not included in the final analysis.

All fMRI data were reconstructed, registered, linear detrended, globally normalized, and then smoothed (10-mm Gaussian kernel). fMRI data were analyzed with SPM2 (www.fil.ion.ucl.ac.uk/spm/software/spm2) as a time series modeled by a sine wave shifted by an estimate of the hemodynamic response. Individual subject maps were created by using *t* statistics (2-Back > 0-Back). These individual contrast images were then used in second-level random effects models to determine task-specific regional responses at the group-level with one-sample *t* tests (main effects of task). To remove anatomical areas not activated in the main task effect, we restricted the second-level random effects analysis to areas that were activated during the task. A functional mask was created from activation maps of 2-Back > 0-Back contrasts ($P < 0.05$, $k = 3$), limiting the analysis to the working memory cortical and subcortical network and controlling for potential differences between the groups arising from areas engaged by only one of the groups. By using this mask, separate ANOVAs with genotype as a grouping factor were performed on 2-Back > 0-Back contrasts. Because of the *a priori* hypothesis of

differential response of striatal regions and working memory cortical network, and use of a rigorous random effects statistical model, we chose a statistical threshold of $P < 0.001$, $k = 3$. Because these areas represented *a priori* brain regions of interest, we corrected the statistical threshold for multiple comparisons with a family-wise error small volume correction (using a 10-mm radius sphere centered on prefrontal and striatal coordinates, $P = 0.01$) (32–34, 36–39). Statistically significant group differences were reported as voxel intensity z values. For anatomical localization, statistical maxima of activation were converted to conform to standard space of Talairach and Tournoux (8).

Working Memory and Attentional Control Tasks. To examine the association with performance on cognitive tasks linked to prefrontal and striatal activity, we used all genotyped 117 subjects who had undergone testing with the N-Back task for working memory ($n = 117$) and the variable attentional control (VAC) task ($n = 105$) (46) (SI Table 5*b*), regardless of any fMRI analysis. The N-Back task included two conditions with increasing loads of working memory, 1-Back and 2-Back. The VAC task also included three conditions with increasing levels of attentional control loads (LOW, MEDIUM, and HIGH). Repeated measures ANOVAs were used to assess the effect of genotype on behavioral performance of working memory and attentional control.

ACKNOWLEDGMENTS. This work was supported by National Institute of Health Research Grants DA022199 and DA021620.

1. Wise RA, Bozarth MA (1987) *Psychol Rev* 94:469–492.
2. Di Chiara G, Imperato A (1988) *Proc Natl Acad Sci USA* 85:5274–5278.
3. Seeman P (2006) *Expert Opin Ther Targets* 10:515–531.
4. Starr MS (1995) *Synapse* 19:264–293.
5. Hallikainen T, Hietala J, Kauhanen J, Pohjalainen T, Syvalahti E, Salonen JT, Tiihonen J (2003) *Am J Med Genet A* 119:152–155.
6. Arinami T, Gao M, Hamaguchi H, Toru M (1997) *Hum Mol Genet* 6:577–582.
7. Lawford BR, Young RM, Swagell CD, Barnes M, Burton SC, Ward WK, Heslop KR, Shadforth S, van Daal A, Morris CP (2005) *Schizophr Res* 73:31–37.
8. Talairach J, Tournoux P (1998) *Co-Planar Stereotaxic Atlas of the Human Brain* (Thieme Medical Publishers, New York).
9. Parsian A, Cloninger CR, Zhang ZH (2000) *Am J Med Genet* 96:407–411.
10. Glatt SJ, Faraone SV, Tsuang MT (2004) *Am J Med Genet B Neuropsychiatr Genet* 128:21–23.
11. Sakai JT, Hopfer CJ, Hartman C, Haberstick BC, Smolen A, Corley RP, Stallings MC, Young SE, Timberlake D, Hewitt JK, Crowley TJ (2007) *Drug Alcohol Depend* 88:130–137.
12. Levy R, Friedman HR, Davachi L, Goldman-Rakic PS (1997) *J Neurosci* 17:3870–3882.
13. Lewis SJ, Dove A, Robbins TW, Barker RA, Owen AM (2004) *Eur J Neurosci* 19:755–760.
14. Owen AM, Doyon J, Petrides M, Evans AC (1996) *Eur J Neurosci* 8:353–364.
15. Newman J, Grace AA (1999) *Conscious Cogn* 8:196–212.
16. Centonze D, Picconi B, Baunez C, Borrelli E, Pisani A, Bernardi G, Calabresi P (2002) *Neuropsychopharmacology* 26:164–175.
17. Delgado A, Sierra A, Querejeta E, Valdiosera RF, Aceves J (2000) *Neuroscience* 95:1043–1048.
18. Cepeda C, Hurst RS, Altemus KL, Flores-Hernandez J, Calvert CR, Jokel ES, Grandy DK, Low MJ, Rubinstein M, Ariano MA, Levine MS (2001) *J Neurophysiol* 85:659–670.
19. Kellendonk C, Simpson EH, Polan HJ, Malleret G, Vronskaya S, Winiger V, Moore H, Kandel ER (2006) *Neuron* 49:603–615.
20. Cropley VL, Fujita M, Innis RB, Nathan PJ (2006) *Biol Psychiatry* 59:898–907.
21. Khan ZU, Mrzljak L, Gutierrez A, de la Calle A, Goldman-Rakic PS (1998) *Proc Natl Acad Sci USA* 95:7731–7736.
22. Usiello A, Baik JH, Rouge-Pont F, Picetti R, Dierich A, LeMeur M, Piazza PV, Borrelli E (2000) *Nature* 408:199–203.
23. Centonze D, Grande C, Usiello A, Gubellini P, Erbs E, Martin AB, Pisani A, Tognazzi N, Bernardi G, Moratalla R, *et al.* (2003) *J Neurosci* 23:6245–6254.
24. Centonze D, Gubellini P, Usiello A, Rossi S, Tscherter A, Bracci E, Erbs E, Tognazzi N, Bernardi G, Pisani A, *et al.* (2004) *Neuroscience* 129:157–166.
25. Yan H, Yuan W, Velculescu VE, Vogelstein B, Kinzler KW (2002) *Science* 297:1143.
26. Zhang Y, Wang D, Johnson AD, Papp AC, Sadée W (2005) *J Biol Chem* 280:32618–32624.
27. Pinsonneault JK, Papp AC, Sadée W (2006) *Hum Mol Genet* 15:2636–2649.
28. Lim JE, Pinsonneault J, Sadée W, Saffen D (2007) *Mol Psychiatry* 12:491–501.
29. Wang D, Johnson AD, Papp AC, Kroetz DL, Sadée W (2005) *Pharmacogenet Genomics* 15:693–704.
30. Duan J, Wainwright MS, Comeron JM, Saitou N, Sanders AR, Gelernter J, Gejman PV (2003) *Hum Mol Genet* 12:205–216.
31. Rogaeva A, Ou XM, Jafar-Nejad H, Lemonde S, Albert PR (2007) *J Biol Chem* 20897–20905.
32. Bertolino A, Blasi G, Latorre V, Rubino V, Rampino A, Sinibaldi L, Caforio G, Petruzzella V, Pizzuti A, Scarabino T, *et al.* (2006) *J Neurosci* 26:3918–3922.
33. Bertolino A, Caforio G, Petruzzella V, Latorre V, Rubino V, Dimalta S, Torraco A, Blasi G, Quartesan R, Mattay VS, *et al.* (2006) *Psychiatry Res* 147:221–226.
34. Bertolino A, Caforio G, Blasi G, De Candia M, Latorre V, Petruzzella V, Altamura M, Nappi G, Papa S, Callicott JH, *et al.* (2004) *Am J Psychiatry* 161:1798–1805.
35. Callicott JH, Mattay VS, Verchinski BA, Marenco S, Egan MF, Weinberger DR (2003) *Am J Psychiatry* 160:2209–2215.
36. Callicott JH, Mattay VS, Bertolino A, Finn K, Coppola R, Frank JA, Goldberg TE, Weinberger DR (1999) *Cereb Cortex* 9:20–26.
37. Postle BR, D'Esposito M (1999) *Brain Res Cogn Brain Res* 8:107–115.
38. Postle BR, Zarahn E, D'Esposito M (2000) *Brain Res Brain Res Protoc* 5:57–66.
39. Chang C, Crottaz-Herbette S, Menon V (2007) *NeuroImage* 34:1253–1269.
40. Minowa T, Minowa MT, Mouradian MM (1992) *Biochemistry* 31:8389–8396.
41. Kamakura S, Iwaki A, Matsumoto M, Fukumaki Y (1997) *Biochem Biophys Res Commun* 235:321–326.
42. Farre D, Roset R, Huerta M, Adsuara JE, Rosello L, Alba MM, Messeguer X (2003) *Nucleic Acids Res* 31:3651–3653.
43. Cartegni L, Wang J, Zhu Z, Zhang MQ, Krainer AR (2003) *Nucleic Acids Res* 31:3568–3571.
44. Pohjalainen T, Rinne JO, Nagren K, Lehikoinen P, Anttila K, Syvalahti EK, Hietala J (1998) *Mol Psychiatry* 3:256–260.
45. Hwang R, Shinkai T, De Luca V, Muller DJ, Ni X, Macciardi F, Potkin S, Lieberman JA, Meltzer HY, Kennedy JL (2005) *Psychopharmacology* 181:179–187.
46. Blasi G, Mattay VS, Bertolino A, Elvevag B, Callicott JH, Das S, Kolachana BS, Egan MF, Goldberg TE, Weinberger DR (2005) *J Neurosci* 25:5038–5045.
47. Papp AC, Pinsonneault JK, Cooke G, Sadée W (2003) *BioTechniques* 34:1068–1072.
48. Wang D, Papp AC, Binkley PF, Johnson JA, Sadée W (2006) *Pharmacogenet Genomics* 16:735–745.
49. Gandelman KY, Harmon S, Todd RD, O'Malley KL (1991) *J Neurochem* 56:1024–1029.
50. Lambert C (2004) HelixTree (Golden Helix, Bozeman, MT).
51. Benjamini Y, Hochberg Y (1995) *J R Stat Soc B* 57:289–300.